

Structure determination, valence, and superexchange in the dimerized low temperature phase of α' - NaV_2O_5

A. Bernert¹, T. Chatterji^{1,2}, P. Thalmeier³, and P. Fulde¹

¹ Max-Planck-Institut für Physik komplexer Systeme, 01187 Dresden, Germany

² Institut Laue-Langevin, BP 156, F-38042 Grenoble Cedex 9, France

³ Max-Planck-Institut für Chemische Physik fester Stoffe, 01187 Dresden, Germany

Published in European Physical Journal B **21**, 535 (2001)

Abstract. We report results of a new analysis for the low-temperature structure of α' - NaV_2O_5 from synchrotron x-ray diffraction experiments. We confirm the existence of two inequivalent ladder structures in each vanadium layer. Based on our structural data we perform a bond-valence calculation for the vanadium sites in the low temperature state. Due to an asymmetric charge ordering we obtain only two different vanadium valences despite the three inequivalent sites. This explains the ^{51}V -NMR observation of only two resonant peaks in the charge ordered phase. By use of a Slater-Koster method to obtain hopping matrix elements and cluster calculations we obtain effective vanadium-vanadium hoppings which compare well to LDA results. Using these in a cluster calculation we obtain a superexchange of 0.047 eV between electrons on neighbouring rungs of the same ladder for the undistorted phase. For the distorted phase we find a significant alternation in the shifts of the oxygen atoms along the legs of one of the two ladder types which leads to a significant exchange dimerisation $\delta_J \approx 0.25$.

PACS. 61.66.Fn Inorganic compounds – 61.50.Ks Crystallographic aspects of phase transformations; pressure effects – 75.30.E Exchange and superexchange interactions

1 Introduction

The layered oxide α' - NaV_2O_5 has attracted great interest since 1996, when Isobe and Ueda reported a phase transition at $T = 34\text{K}$ with a spin-Peierls like spin gap formation [1]. An earlier determination of the high-temperature structure [2] originally reported two inequivalent vanadium sites. However, a redetermination of the crystal structure of the high-temperature phase found the space group Pmmn [3,4,5] instead of $\text{P2}_1\text{mn}$, with only one type of vanadium site. Due to stoichiometry this site should have a valence of +4.5. Later, a ^{51}V -NMR study by Ohama et al [6] reported the existence of two inequivalent vanadium sites below the critical temperature. This is supposed to be caused by a charge ordering transition of the material which leads to inequivalent vanadium atoms with different valences. A determination of the low-temperature structure by x-ray scattering then reported [7] *three* inequivalent vanadium sites. Using this data a bond-valence calculation then led to three different valences, [8] approximately given by +4, +4.5, and +5, in contrast to the result of the ^{51}V -NMR measurements.

In this article, we will give the results of a determination of the low-temperature structure using a much larger data set than used in [7]. Applying bond-valence analysis to our data we obtain only *two* significantly different

valences for the vanadium sites, despite the fact that our structural data show also three inequivalent sites.

Due to shifts in the oxygen positions we further find an alternation in the exchange coupling constant between the vanadium sites on one type of ladder and give an estimate for the corresponding exchange dimerisation parameter δ_J .

This article is organised as follows. In the next section we present the experimental details and the results of the structure determination. We find three inequivalent vanadium sites in each layer, building two inequivalent vanadium-oxygen ladders per layer. In the third section we use the bond-valence method to determine the valences of the sodium and the vanadium atoms both in the undistorted and the distorted phase and compare the results with the observations of NMR. In the fourth section we look at the superexchange coupling along ladder direction for the undistorted phase and for the two ladders per layer of the distorted phase. To do this we first determine approximate vanadium-oxygen and sodium-oxygen hopping matrix elements. From these we find the effective vanadium-vanadium hopping elements by use of a block diagonalization comparing our results with those of a recent LDA calculation [9]. We proceed to find the superexchange coupling for the different ladder types and deter-

Table 1. Average structure parameters obtained by using fundamental reflections at 15K.

Site	x	y	z	Site	x	y	z
V	0.40212(7)	0.25000(0)	0.39067(22)	Na	0.25000(0)	-0.25000(0)	0.85362(73)
O ₁	0.25000(0)	0.25000(0)	0.51111(122)	O ₂	0.38565(42)	0.25000(0)	1.05413(151)
O ₃	0.42595(39)	-0.25000(0)	0.50381(93)	Cell [13]	11.3030(1)Å	3.61095(3)Å	4.7525(1)Å

mine its alternation along the ladder direction. In the last section we summarize and discuss our results.

2 Structure details

The crystal structure of the room temperature phase of NaV_2O_5 based on X-ray diffraction intensity data has been reported previously [3]. We have measured the diffraction intensities of NaV_2O_5 at $T = 15$ K in the charge ordered phase using the same crystal. The experiment was performed using a single crystal of size $0.03 \times 0.09 \times 0.20$ mm³ on the diffractometer D3 at the synchrotron X-ray source of the HASYLAB at DESY, Hamburg by using X-ray wavelength $\lambda = 0.559\text{\AA}$. The sample was mounted inside a Displex cooling device attached to the four-circle diffractometer. The superlattice reflections were detected corresponding to the lattice parameters $a = 2 \times a_0$, $b = 2 \times b_0$ and $c = 4 \times c_0$ where a_0 , b_0 and c_0 are subcell lattice parameters. To determine the space group, reflections were measured using the primitive super cell for small values of Bragg angles which showed that the space group is $Fmm2$. 4847 reflections were measured at $T = 15\text{K}$ up to $\sin \theta / \lambda = 0.94\text{\AA}^{-1}$ which gave rise to 1953 unique reflections. We have determined the average structure by using only the fundamental reflections and the room temperature structure model in space group $Pm\bar{m}n$. Least-squares refinement of the crystal structure by using SHLEX program led to the atom parameters listed in table 1. The residual index R , defined as

$$R = \frac{\sum ||F_0| - |F_c||}{\sum |F_0|} \quad (1)$$

was $R = 0.060$. The average structure obtained agrees closely with the room temperature structure [3] as expected. We next refined the charge-ordered distorted low temperature structure in the space group $Fmm2$. The number of parameters refined were 61. The starting parameters were the parameters of the average structure (table 1) transformed appropriately to the supercell. The resulting atom coordinates have been given in table 2. Note that contrary to the superspace group refinement of reference [7] we have employed the standard crystallographic refinement procedure which we could afford due to the very large number of reflection intensities measured up to a large value of $\sin \theta / \lambda = 0.94\text{\AA}^{-1}$. Accordingly our parameters were free from the constraints of the refinement using the superspace group. Our refinement also led to physically meaningful thermal parameters. The residual index was $R = 0.056$. The atom coordinates are listed in table 2. To

ensure that the refinement did not lead to a local minimum we used the so-called multistart-and-refine procedure in which one starts from several initial displaced coordinates. These refinements lead to identical coordinates within the standard deviations. Recently doubts have been raised about the the actual space group of NaV_2O_5 . ²³Na-NMR results have suggested a lower-symmetry space group than $Fmm2$ [10]. We did not attempt to refine the crystal structure by lowering the space group symmetry because of the very large number of parameters and consequent strong correlations among the parameters involved. Also there exists no diffraction evidence for a lower symmetry space group. Details of the present refinement procedure will be published elsewhere [11].

We get the same qualitative results as were found in [7, 12]. Two slightly different types of vanadium layers were found. Both layers look similar as shown in figure 1 with three inequivalent sites and as described in [7]. We denote the two different layers by the subscripts a and b and the vanadium sites as shown in figure 1. Apart from the slightly different magnitude of the shifts the main qualitative difference is, that for layer a the V_{1a} sites shift in b direction towards the V_{21a} sites while for layer b the V_{1b} sites are found to shift away in b-direction from the V_{21b} sites.

3 Bond-valence calculation

The bond-valence method serves to determine the valences of atoms in a chemical compound [14]. The valence of an atom in a compound, as determined by this method, is the sum of the bond valences for all bonds, in which the atom participates. The bond valences of such anion-cation bonds are empirically defined as

$$v_i = \exp [(r_0 - r_i) / B], \quad (2)$$

where B is fixed to be 0.37. r_i is the distance between the two atoms of the anion-cation bond, r_0 is an empirical parameter obtained from fitting the atomic valences for many different compounds at room temperature [15]. There is an alternative definition for the bond valence, namely

$$v_i = \left(\frac{r_i}{r_0} \right)^{-N}, \quad (3)$$

where both r_0 and N are empirical parameters. Both definitions give similar results; we will adopt definition (2) throughout this article, as this method was also used in [8].

It should be noted that the bond valence model does not imply a certain physical nature of the bond. It works

Table 2. Low temperature phase structure at $T = 15$ K and shifts from high temperature structure as given in [3]. Size of unit cell taken from [13]. Shifts from the positions in [3] have been calculated after shifting the low temperature unit cell by the vector $(-1/8, 1/8, 0.87959/4)$. The shift in z direction is chosen, such that the positional change of V2 and V4 is nearly zero and symmetrical. Thus, the vanadium sites of the spin dimerised ladders do not move in z direction below T_C .

Site	Coordinates			Shift (new-old)		
	x	y	z	Δx	Δy	Δz
V1 (V_{21a})	0.32777(15)	0.00000(0)	-0.06039(19)	0.00172	0.00000	-0.00336
V2 (V_{1a})	0.07595(6)	0.24992(3)	0.49682(8)	-0.00011	-0.00008	-0.00001
V3 (V_{22b})	0.32460(16)	0.00000(0)	0.19398(23)	-0.00146	0.00000	0.00102
V4 (V_{1b})	0.07611(6)	0.25013(3)	0.24684(8)	0.00006	0.00013	0.00001
V5 (V_{22a})	0.32469(17)	0.00000(0)	0.44451(19)	-0.00137	0.00000	0.00155
V6 (V_{21b})	0.32771(16)	0.00000(0)	0.69017(24)	0.00166	0.00000	-0.00280
Na1	0.25000(0)	-0.25000(0)	-0.19233(32)	0.00000	0.00000	-0.00205
Na2	0.25000(0)	-0.25000(0)	0.05830(32)	0.00000	0.00000	-0.00142
Na3	0.00000(0)	0.00000(0)	0.13004(30)	0.00000	0.00000	-0.00003
Na4	0.00000(0)	0.00000(0)	0.38016(29)	0.00000	0.00000	0.00009
Na5	0.00000(0)	0.50000(0)	0.37925(30)	0.00000	0.00000	-0.00082
Na6	0.00000(0)	0.50000(0)	0.12955(31)	0.00000	0.00000	-0.00052
O1	0.25133(11)	0.00000(0)	0.22409(48)	-0.00133	0.00000	0.00053
O2	0.24930(15)	0.00000(0)	-0.02628(52)	-0.00070	0.00000	-0.00090
O3	0.00000(0)	0.25299(34)	0.46549(50)	0.00000	0.00299	0.00032
O4	0.00000(0)	0.25283(35)	0.21551(50)	0.00000	0.00283	0.00034
O5	0.08905(29)	0.50000(0)	0.21785(35)	0.00050	0.00000	0.00098
O6	0.08763(28)	0.00000(0)	0.46609(33)	-0.00092	0.00000	-0.00078
O7	0.33823(28)	0.24747(20)	0.22238(31)	-0.00032	-0.00253	-0.00054
O8	0.33865(29)	-0.25153(28)	-0.02744(31)	0.00010	-0.00153	-0.00036
O9	0.08746(28)	0.00000(0)	0.21637(34)	-0.00109	0.00000	-0.00050
O10	0.08914(29)	0.50000(0)	0.46812(33)	0.00059	0.00000	0.00125
O11	0.31682(28)	0.00000(0)	0.10863(37)	-0.00103	0.00000	-0.00072
O12	0.31636(27)	0.00000(0)	-0.14520(31)	-0.00149	0.00000	-0.00455
O13	0.31669(28)	0.00000(0)	0.60519(35)	-0.00116	0.00000	-0.00416
O14	0.31686(27)	0.00000(0)	0.35913(32)	-0.00099	0.00000	-0.00022
O15	0.06871(29)	0.24749(18)	0.58013(31)	0.00086	-0.00251	-0.00032
O16	0.06979(29)	0.24890(27)	0.33107(34)	0.00194	-0.00110	0.00062
Cell	$2 \times 11.3030(1)\text{\AA}$	$2 \times 3.61095(3)\text{\AA}$	$4 \times 4.7525(2)\text{\AA}$			

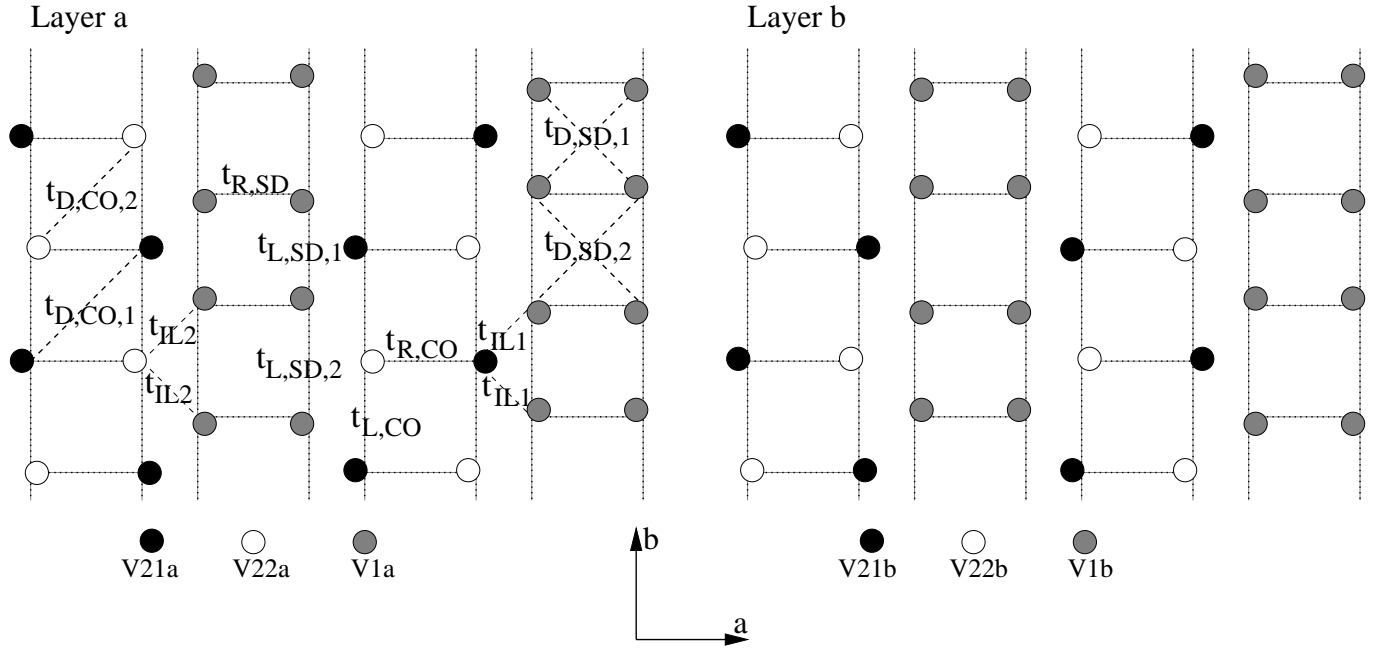


Fig. 1. Vanadium layer of the low-temperature structure. Note the difference in the shifts of V_{1a} and V_{1b} . Figure not to scale.

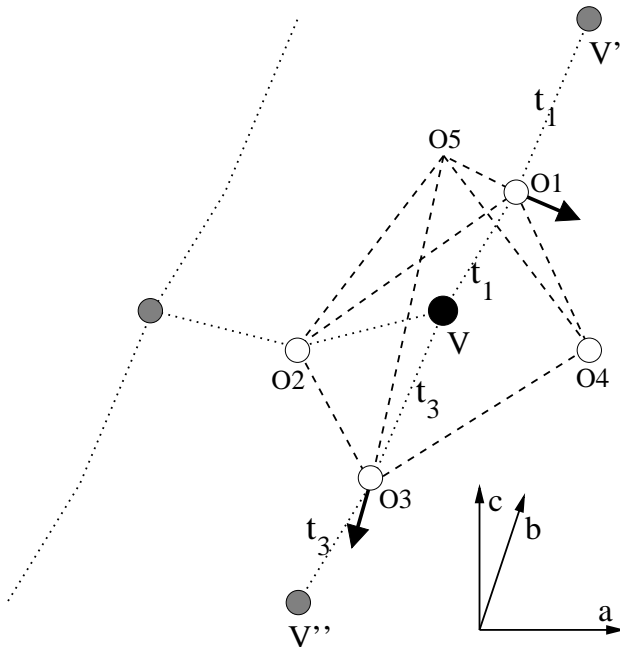


Fig. 2. Oxygen (white) and vanadium atoms (grey) around vanadium atom (black) on same ladder. Arrows indicate shift of oxygen atoms along the leg in the V_1 -ladders. Figure not to scale.

both with covalent and ionic type bonds [16]. Inaccuracies generally come from two sources: First, the errors of the structure determination and the lattice constant determination. Second, the inaccuracy of the parameter r_0 in (2). This parameter is determined from fitting it to a large number of structures containing a given bond type and therefore carries an error with it. We give the total standard deviation derived from these two sources of errors in our results for the valences. In our calculations for the vanadium site valences the inaccuracies from the structure determination and the lattice constant play the leading role.

Therefore, in a first step we use the method to determine the valences of the atoms in the undistorted phase. This enables us to adjust parameters to account for the peculiarities of the material as well as to estimate the accuracy of the method. In a second step we determine the valences of the vanadium and sodium atoms in the distorted phase. This will give us some insight into likely charge order structures.

3.1 Atomic valences in the undistorted phase

We have obtained the bond lengths for the vanadium-oxygen bonds and the sodium-oxygen bonds from the structural data in [3] and give them in tables 3 and 4.

Using the lengths of the vanadium-oxygen bonds we determine the valences of the vanadium and the sodium atoms in the undistorted phase by 2. Using room temperature lattice parameters and the empirical r_0 given in [15] we obtain two different results, depending on which

Table 3. Vanadium-oxygen bond lengths given in Ångström. V_0 denotes the vanadium site of the undistorted phase. For the nomenclature of the oxygen sites, see figure 2. The first row gives the distances for room temperature lattice parameters as given in [3], the second row gives distances for lattice parameters at 15K — see table 2.

	O_1	O_2	O_3	O_4	O_5
V_0	1.916(3)	1.825	1.916(3)	1.986(3)	1.616(3)
V_0	1.914(3)	1.8216(7)	1.914(3)	1.983(3)	1.600(3)

Table 4. Sodium-oxygen bond lengths given in Ångström for room temperature lattice constants (first row) and lattice constants at 15K (second row). Na_0 denotes the sodium site of the undistorted phase; for the nomenclature of the oxygen sites see figure 3. Due to symmetry there are always pairs of bonds with the same length, thus, the lengths of only four bonds are given.

	O_R	O_L	O_{A1}	O_{A2}
Na_0	2.435	2.606	2.554	2.554
Na_0	2.424	2.594	2.550	2.550

value we take for r_0 . Using the value for V^{4+} -O bonds $r_{4+} = 1.784(27)\text{Å}$ gives a valence of 4.45; using the value for V^{5+} -O bonds $r_{5+} = 1.803(31)\text{Å}$ leads to a valence of 4.69. We know from stoichiometry that the vanadium atom should have a valence of 4.5. Just using the average of the two r_0 given above is not a good approximation, since the characteristic bond lengths do not vary linearly with the bond order. Therefore, we use a fitted $r_{4.5+} = 1.788(5)\text{Å}$ to give the correct valence 4.5 for the undistorted phase with room temperature lattice parameters.

The size of the unit cell decreases significantly from 300K to 15K. We therefore cannot simply use the r_{4+} , $r_{4.5+}$ and r_{5+} from above, since they result from room temperature structure determinations. Using the high temperature $r_{4.5+}$ with the low temperature lattice parameters for determination of the valence of the vanadium site in the undistorted phase would give a valence of 4.59. We therefore have to scale down all these characteristic bond lengths. For this scale we use the factor $(V_{15K}/V_{300K})^{1/3} = 0.9965$ where the V are the volumes of a cell containing four vanadium sites. We then obtain a valence of 4.51 for the vanadium atom in the undistorted phase using low temperature lattice constants and the reduced $r_{4.5+}$.

We can follow through a similar exercise for the sodium atom. We find that the characteristic bond length $r_{Na} = 1.803\text{Å}$ given in [15] gives a valence of 1.12 for the sodium atom in the undistorted phase with room temperature lattice parameters, which is clearly deviating strongly from the expected value 1. It is known, however, that there is a comparatively strong physical variation in the environment of alkali atoms, therefore the characteristic bond lengths vary strongly, the standard deviation being about 0.08Å [15]. It is therefore justified to use a characteristic bond length $r_{Na} = 1.762(5)\text{Å}$ obtained by fitting the resulting valence to 1. This helps capturing the special

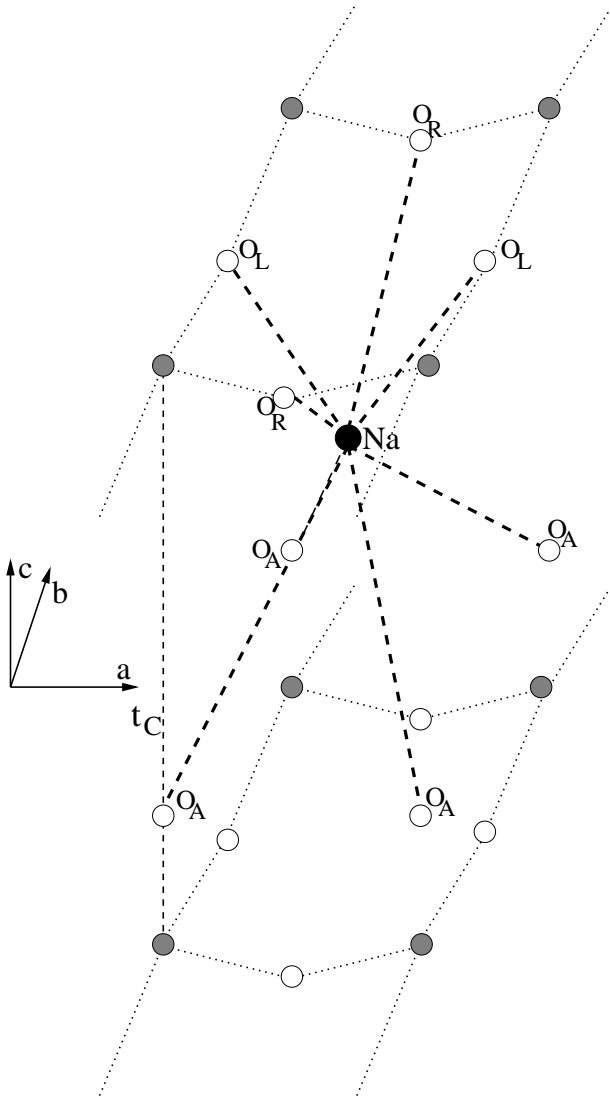


Fig. 3. Sodium (black), oxygen(white) and vanadium (grey) atoms on two ladders in two neighbouring layers. Figure not to scale.

physical features of the environment surrounding the alkali atom in this material. Scaling down this characteristic r_{Na} to 1.756(5) for lattice constants at 15 K as in the case of vanadium and using these lattice constants we arrive at a valence of 1.00(1) for the sodium atom in the undistorted phase using low temperature lattice parameters. Since r_{Na} is a fitted value, the error comes only from the standard deviation of the structure determination and is much smaller than the standard deviation of r_{Na} from [15]. All the parameters used are listed in table 5. Henceforth we will always use the lattice parameters and characteristic bond lengths for temperature 15K as given there.

To check the quality of the bond valence method we now determine the valence of the three oxygen sites of the undistorted phase. Since the bond orders are already determined, the total valence of the five oxygen atoms in a unit cell is $-10.02(6)$, corresponding to the total valence of

Table 5. Parameters used for the determination of atomic valence. Lattice constants from [3,13], for other parameters see text.

	T= 300K	T= 15K
a	11.311 Å	11.3030 Å
b	3.6105 Å	3.61095 Å
c	4.800 Å	4.7525 Å
r_{4+}	1.784(5) Å	1.778(27) Å
$r_{4.5+}$	1.788(5) Å	1.782(5) Å
r_{5+}	1.803(3) Å	1.797(31) Å
r_{Na}	1.762(5) Å	1.756(5) Å
V	196.0 Å ³	194.0 Å ³

the cations. However the valence of the different oxygens is not the nominal value -2 for each as might be expected. Instead we obtain a valence of $-1.87(2)$ for the apical oxygen, $-2.08(2)$ for the oxygen on the leg of the V-O-ladder, and $-2.12(2)$ for the oxygen on a rung. Qualitatively this may be explained with the fact that the oxygen atoms are easily polarizable.

3.2 Atomic valences in the distorted phase

We will now determine the valence of the vanadium and the sodium atoms in the distorted phase at 15K. For this we will use parameters as given in table 5.

The bond lengths of the vanadium-oxygen bonds and of the sodium-oxygen bonds as well as the valences resulting are listed in tables 6 and 7. Due to the fact that the exact valence of the vanadium atoms is not known a priori and that the characteristic bond length r_0 depends on this valence, one has to use a self consistency procedure to derive the valences for the vanadium atoms as given in the last column of table 6.

Regarding the sodium atom valence one observes, that the changes of valence are smaller than the standard deviation, which is mostly due to the standard deviation of r_{Na} . Furthermore the average valence does not change significantly, it is equal to 1.01(3).

Regarding vanadium, the first observation is that the valences of similar vanadium atoms in the two layers are not the same within one standard deviation. We will therefore look at these layers separately.

We first look at the valences for layer a . Although the V_{1a} and the V_{22a} sites are crystallographically inequivalent they have approximately the same valence 4.6. The V_{21a} site has a lower valence of approximately 4.1. Note that the shift from the average valence 4.5 is significantly different for V_{21a} and V_{22a} .

For layer b the results are somewhat different. Here the V_{1b} site experiences only a small change of valence. Despite this the absolute size of the valence shifts from the original average valence 4.5, which are 0.43(4) for V_{21b} and 0.19(4) for V_{22b} , are significantly different from each other.

To determine the quality of the results, one can calculate the stoichiometrically averaged valence of a vana-

Table 6. Vanadium-oxygen bond lengths given in Ångström and valences in the distorted phase at 15K. Nomenclature for atoms as given in figures 2 and 1. For the valences The first three columns show the valence depending on the characteristic bond length r_0 used, the last row gives values which are self-consistent to first order.

	O ₁	O ₂	O ₃	O ₄	O ₅	Valences			SC
						r ₄₊	r _{4.5+}	r ₅₊	
V _{1a}	1.910(2)	1.817(4)	1.915(3)	1.985(7)	1.592(6)	4.51(4)	4.56(4)	4.75(4)	4.60(4)
V _{21a}	1.937(4)	1.889(8)	1.937(4)	1.978(7)	1.633(5)	4.11(4)	4.15(4)	4.32(4)	4.12(4)
V _{22a}	1.898(3)	1.762(9)	1.898(3)	1.999(7)	1.633(5)	4.52(4)	4.57(4)	4.76(4)	4.61(4)
V _{1b}	1.914(3)	1.821(4)	1.909(3)	1.992(7)	1.608(7)	4.43(4)	4.48(4)	4.66(4)	4.48(4)
V _{21b}	1.938(3)	1.900(7)	1.938(3)	1.981(7)	1.635(6)	4.07(4)	4.11(4)	4.28(4)	4.07(4)
V _{22b}	1.892(3)	1.752(7)	1.892(3)	2.004(7)	1.632(6)	4.57(4)	4.62(4)	4.81(4)	4.69(4)

Table 7. Sodium-oxygen bond lengths given in Ångström and valence in the distorted phase at 15K. Nomenclature for oxygen atoms as shown in figure 3. Due to symmetry there are pairs of bonds of equal length, only one of each pair is given.

	O _R	O _L	O _{A1}	O _{A2}	Valence
Na1	2.405	2.570	2.513	2.550	1.06(8)
Na2	2.418	2.583	2.541	2.515	1.04(8)
Na3	2.444	2.569	2.576	2.576	0.97(8)
Na4	2.443	2.568	2.567	2.567	0.98(8)
Na5	2.423	2.630	2.572	2.572	0.96(8)
Na6	2.420	2.621	2.548	2.548	1.00(8)

dium site for the low-temperature structure. Due to charge conservation one would ideally expect an average valence of 4.5. Using the self-consistently interpolated values one obtains 4.48(2) for layer *a* and 4.43(2) for layer *b*. This indicates that the results for layer *a* should be the more reliable. The difference between the results for the different layers can well be caused by the refinement method of the structure determination, which might have found a less reliable local minimum for layer *b* than for layer *a*. From these bond valence calculations for layer *a* we therefore conclude that there are *only two* significantly different vanadium valences in the distorted phase, contrary to the result of van Smaalen and Lüdecke, who obtained three clearly different valences [8] and a nearly symmetrical charge shift between the V₂₁ and the V₂₂ sites. However, in our analysis we obtain a significantly asymmetrical charge shift between the V₂₁ sites on one hand and the V₁ and V₂₂ sites on the other hand for both layers.

Such a charge transfer between ladders does not have to cause the material to become a conductor. The insulating behaviour of the high temperature phase has been explained with correlation effects, due to which one can map the quarter filled ladder to a half-filled Hubbard chain [17], resulting in an effective charge transfer gap. Since this argument works only at quarter-filling, one might expect the material to become a conductor if a charge transfer takes place between ladders as described above. While this is true if one considers isolated ladders, the situation becomes less simple if inter-ladder Coulomb repulsion is included in the model, due to the geometry of the lattice. Consider a hexagon of V₁ and V₂₂ sites and assume that

the V₂₁ sites carry one electron each. In this case one has two electrons for each six other sites, close to what is found from bond valence above. As a consequence, one still has a charge transfer gap, because due to the geometry of the lattice it is not possible to put three electrons on such a hexagon without having Coulomb repulsion. Therefore depending on the ratio of the parameters involved, the system can still be a charge transfer insulator.

3.3 Comparison with NMR

We can compare our result to the results of the ⁵¹V-NMR measurements [6]. For such a measurement one expects that the resonant peak for the high-temperature vanadium site with valence +4.5 splits into multiple peaks below the transition: one peak for each different valence of vanadium sites is expected. The intensity of a peak for a given valence should be approximately proportional to the number of vanadium sites having such valence.

The interaction between the 3d electrons and the nuclei of the vanadium which causes the shift of the NMR resonance frequency, is, disregarding crystal field effects due to the distortion, roughly proportional to the density of the *d_{xy}*-electrons on a shell of a given vanadium ion. Therefore one expects that the splitting of the resonant NMR-peak at the transition temperature reflects the charge disproportionation approximately linearly, at least close to the critical temperature.

For a low-temperature structure with three different valences $4.5 - \delta$ for the V₂₁ sites, 4.5 for the V₁ sites, and $4.5 + \delta$ for the V₂₂ sites, as suggested by [8], one expects a splitting of the single high-temperature resonant peak into *three* different peaks with an intensity ratio of approximately 1 : 2 : 1, the corresponding shifts of the right and left peak should be roughly symmetrical around the center peak and the center peak in continuation of the single high temperature resonance peak. For a low-temperature structure with only two different valences $4.5 - 3\delta$ for the V₂₁ sites, and $4.5 + \delta$ for the V₂₂ and the V₁ sites as suggested by our analysis above, one expects a splitting of the high-temperature resonant peak into *two* peaks at the transition temperature with an intensity ratio of approximately 1 : 3 and where the shifts of the new peaks from the old peak obey a 3 : 1 ratio.

Looking at the experimental results as given in figure 3 of [6], one finds, that *two* resonant peaks have been found below 33.4K. The shift of these two peaks relative to the high-temperature peak is clearly asymmetric, and the ratio of the distances is roughly 2 : 1 in favour of the left peak which has been identified to be a V^{4+} resonant peak by the authors. The ratio of the intensities, as determined by the area below the peaks, is roughly 1 : 3 from 30K to 33.3K. This changes at 20K, but it is not mentioned in [6] whether intensity correction has been performed for the data, so as far as intensity ratios are concerned we use only the data around T_C .

From 33.4K to 33.6K three peaks are found. One of them is clearly the continuation of the high-temperature peak for valence 4.5. This behaviour might be intrinsic or due to a distribution of the T_C in the powder sample used for the measurement. In the former case (intrinsic behaviour) one would identify the center peak with the V_1 sites and the left and right peak with the V_{21} and the V_{22} sites, respectively. Since the charge of the V_1 sites would then remain constant in this temperature interval, the charge shift of the V_{21} and the V_{22} sites would be of the same amount and different sign. This implies a ratio of roughly 1 : 1 for the distances of the two side peaks from the center peak, i.e., a different ratio than that measured below 33.4K. For the latter case (distribution of T_C) one would not expect a big change of the distance ratio at 33.4K. Since one finds that the ratio of distances is still 2 : 1 from 33.4K to 33.6K, we believe that the observation of three peaks is due to a distribution of the T_C rather than intrinsic. However, below 33.4K the ^{51}V -NMR measurements seem to be in much better agreement with the results of our analysis, yielding *only two* different valences with an asymmetrical charge disproportionation, than with the previous analysis of van Smaalen and Lüdecke yielding *three* different valences and symmetrical charge disproportionation [8]. Our results also explain, that the low-valence V_{21} sites can have a valence of nearly 4 as determined in [6] from the hyperfine coupling strengths, although the charge disproportionation δ_C in the system is estimated to be small: $\delta_C \ll 0.5$ [18, 19].

4 Exchange coupling constant alternation

From the structural data we observe a slight alternation in the distances in b-direction between V_1 sites for the V_1 ladder in both layers. The lattice dimerisation parameter δ_V for the shift of the V_1 sites in b direction is very small with 0.04% for layer *a* and 0.05% for layer *b* compared to 0.56% for CuGeO_3 [20]. However, even a small alternation implies an alternation in the exchange coupling in b-direction.

Under the assumption that the observed spin-gap results from an alternation of the exchange coupling in *all* ladders, the exchange dimerization parameter $\delta_J = (J_+ - J_-)/(J_+ + J_-)$ is estimated to lie between 3.4% to 10% for α' - NaV_2O_5 [21, 22, 23, 24] and 3% to 17% for CuGeO_3 [20, 25]. In both cases the higher values result from mean-field estimates, which might be insufficient for a treatment of

these materials as argued for α' - NaV_2O_5 in [21]. However, the assumption that there is an exchange coupling alternation in all ladders of the distorted phase is flawed from the point of structure determination, since we observe only for the V_1 -ladders any alternation in b-direction, but not for the V_{21} - V_{22} -ladders.

Assuming that an alternation of the exchange coupling in b-direction takes place only in every second ladder, a recent theoretical study estimated the dimerisation parameter δ necessary to produce the observed size of the spin gap as $\delta \approx 0.38 \dots 0.54$. [26] This would be even larger than the dimerisation observed in CuGeO_3 . Thus, it seems unlikely, that the shifts of the vanadium sites and the resulting dimerisation in α' - NaV_2O_5 which is an order of magnitude smaller than that for CuGeO_3 should give an exchange dimerisation of the same order of magnitude.

However, the small dimerisation of the vanadium sites is not the only alternation along the legs of the V_1 ladders. One finds a much stronger alternation in the distances to the nearest oxygen atoms which are on the same leg as the V_1 atom in question. This alternation results from the shift of these oxygen atoms in a- and c-direction. For the V_{21} - V_{22} ladder no effective alternation in b-direction is found, neither from shifts of the oxygen sites nor from shifts of the vanadium sites.

It is possible to determine the exchange dimerisation parameter from the structural data. Let us first give a very simple estimate. For the superexchange interaction between rungs we have approximately $J \propto t_{VV}^2$, $t_{VO} \propto t_{VO}^2$, and, according to [27], $t_{VO} \propto d_{VO}^{-3.5}$. t_{VO} is a hopping matrix element between the vanadium d_{xy} -orbital and the p-orbital of the neighbouring oxygen on the same rung. t_{VV} is therefore an effective hopping matrix element between neighbouring vanadium sites of on the same leg of a ladder. This implies, that for small distortions which change the distance d_{VO} by $\pm \Delta d_{VO}$ we obtain $\delta_J = \Delta J/J \approx \pm 14 \Delta d_{VO}/d_{VO}$. For the vanadium-oxygen bond lengths between atoms on the same leg of the V_1 ladder given in table 6, one finds $\delta_J \approx 2\%$. This is one order of magnitude larger compared to what one would have obtained by using the shifts of the vanadium sites only.

We will now first examine the hopping matrix elements for the undistorted phase, calculating them with the method presented in [28] using the parameters from [27]. From this we will gain insight in the effective t_{VV} hopping matrix elements and the effective superexchange between rungs on the same ladder. In a second step we extend this method onto the distorted phase to find the approximate size of the superexchange dimerisation on the V_1 ladders.

4.1 Hopping and superexchange in the undistorted phase

We determine the matrix elements for the electron hopping by a Slater-Koster type of treatment presented in [27] and [28]. We will use hopping matrix elements along anion-cation bonds and between vanadium orbitals only. For the vanadium sites, we consider only the lowest lying 3d-orbital, which is the d_{xy} orbital according to [9]. For the

Table 8. Distances (in Ångström) between vanadium and oxygen atoms and hopping matrix elements (in eV) between vanadium d_{xy} and oxygen p-orbitals for the undistorted phase. The absolute values of the hoppings and the distances are given, the sign is determined by the orientation of the vector between the vanadium and the oxygen site. Denomination of oxygen atoms as in figure 2. $\text{O}_{5'}$ denotes the apex oxygen of the VO_5 pyramid lying above or below the central vanadium site.

	Δx	Δy	Δz	d_{VO}	$t_{p_x d_{xy}}$	$t_{p_y d_{xy}}$	$t_{p_z d_{xy}}$
O_1, O_3	0.2825	1.8055	-0.5695	1.914	0.8549	0.6303	0.2470
O_2	1.7193	0	0.6018	1.822	0	1.1632	0
O_4	1.9304	0	0.4545	1.983	0	0.8909	0
O_5	0.1855	0	1.5896	1.600	0	0.2247	0
$\text{O}_{5'}$	0.1855	0	3.1629	3.168	0	0.0104	0

Table 9. Distances (in Ångström) between sodium and oxygen atoms and hopping matrix elements (in eV) between sodium 3s and oxygen p-orbitals for the undistorted phase. The absolute values of the hoppings and the distances are given, the sign is determined by the orientation of the vector between the vanadium and the oxygen site. Denomination of oxygen atoms as in figure 2.

	Δx	Δy	Δz	d_{NaO}	t_{sp_x}	t_{sp_y}	t_{sp_z}
$\text{O}_{A1}, \text{O}_{A2}$	1.5338	1.8055	0.9434	2.550	1.2970	1.5267	0.7977
O_L	2.0018	0	1.6501	2.594	1.6076	0	1.3252
O_R	0	1.8055	1.6178	2.424	0	1.7768	1.5921

oxygen sites we use the 2p-orbitals, assuming them to be of equal energy, while for the sodium sites we use the 3s-orbital. In this case, the hopping between vanadium and oxygen sites is [28, 27]

$$\begin{aligned}
 t_{p_x d_{xy}} &= m \left(\sqrt{3} l^2 V_{pd\sigma} + (1 - 2l^2) V_{pd\pi} \right) \\
 t_{p_y d_{xy}} &= l \left(\sqrt{3} m^2 V_{pd\sigma} + (1 - 2m^2) V_{pd\pi} \right) \\
 t_{p_z d_{xy}} &= lmn \left(\sqrt{3} V_{pd\sigma} - 2V_{pd\pi} \right)
 \end{aligned} \quad (4)$$

with l, m, n being the direction cosines of the vector from the p state to the d state and the parameters

$$\begin{aligned}
 V_{pd\sigma} &= -21.808 \text{ eV} \text{Å}^{7/2} d_{VO}^{-7/2}, \\
 V_{pd\pi} &= 10.054 \text{ eV} \text{Å}^{7/2} d_{VO}^{-7/2}.
 \end{aligned}$$

The matrix elements for the Na-O hopping are determined from

$$\begin{aligned}
 t_{sp_x} &= lV_{sp\sigma}, \\
 t_{sp_y} &= mV_{sp\sigma}, \\
 t_{sp_z} &= nV_{sp\sigma}, \\
 V_{sp\sigma} &= 14.0208 \text{ eV} \text{Å}^2 d_{NaO}^{-2}.
 \end{aligned}$$

Finally we may also consider hopping between nearest neighbour vanadium sites on different rungs. In this case the matrix elements are given by

$$t_{d_{xy} d_{xy}} = 3l^2 m^2 V_{dd\sigma} + (l^2 + m^2 - 4l^2 m^2) V_{dd\pi} \quad (5)$$

with parameters

$$\begin{aligned}
 V_{dd\sigma} &= -116.18 \text{ eV} \text{Å}^5 d_{VO}^{-5}, \\
 V_{dd\pi} &= 62.754 \text{ eV} \text{Å}^5 d_{VO}^{-5}.
 \end{aligned}$$

The coordinate differences, distances and resulting hopping elements between the sites are given in tables 8 and 9. For the direct d_{xy} - d_{xy} hopping matrix element one obtains 0.2231 eV in the undistorted phase.

Using these matrix elements, we will now proceed to determine effective vanadium-vanadium hopping in the following way. Consider the single particle Hamiltonian H_{SP} of the problem. In matrix notation it has the form

$$\mathbf{H}_{SP} = \begin{pmatrix} \mathbf{T}_{VV} & \mathbf{T}_{VO} & \mathbf{T}_{VNa} \\ \mathbf{T}_{OV} & \mathbf{T}_{OO} & \mathbf{T}_{ONa} \\ \mathbf{T}_{NaV} & \mathbf{T}_{NaO} & \mathbf{T}_{NaNa} \end{pmatrix}. \quad (6)$$

The on-site energies ϵ_V , ϵ_O , and ϵ_{Na} on the diagonal of \mathbf{T}_{VV} , \mathbf{T}_{OO} , and \mathbf{T}_{NaNa} are given in [27] as $\epsilon_V = -12.55$ eV, $\epsilon_O = -14.13$ eV, $\epsilon_{Na} = -5.13$ eV. One observes, that the hopping from one layer to another via the intermediate apex oxygen is very small. However, this is not so clear for hopping via the path V-O₁-Na-O₅-V. Therefore to find effective vanadium-vanadium hopping matrix elements we block-diagonalize \mathbf{H} given above with successive Jacobi transformations, projecting out the sub-matrices \mathbf{T}_{VO} , \mathbf{T}_{NaO} and their conjugates to separate the Hilbert space of the vanadium orbitals from that of the rest. We then proceed to use these effective vanadium-vanadium hoppings as parameters of an extended Hubbard model describing the system.

The block diagonalization is done for a cluster of 4 layers by 4 rungs by 4 ladders. The resulting values for the effective hoppings can be found in table 10 and we can compare them with the results from an LDA tight-binding fit presented in [9]. The results are partly similar: t_R is larger than both t_L and t_D , although all these values are smaller than those from LDA. t_L and t_R are of similar size. t_C , the effective hopping between layers, is much smaller than all other effective hoppings in both cases.

Table 10. Effective vanadium-vanadium hoppings for the undistorted phase given in eV. Denomination of hoppings as given in figure 1. For methods see text. Superexchange J_{eff} has been calculated with $U = 4$ eV, and $V_L = 2t_R$ as given (see text).

Method	t_R	t_L	t_D	t_{IL}	t_c	V_L	J_{eff}
LDA [9]	0.38	0.085	0.085	—	—	0.76	0.070
Ab initio [29]	0.5382	0.1246	—	-0.0442	—	1.076	0.038
All hoppings	0.172	0.049	0.062	-0.110	0.009	0.344	0.047
Without Na-O	0.305	0.100	0.016	-0.111	< 0.001	0.610	0.044

We can also compare our values with the results from an ab-initio calculation using the DDCI2 quantum chemical method as presented in [29]. They obtain a t_R which is larger than ours or that from LDA calculation. They do not obtain a value for t_D because Na orbitals were not included in their calculation. Therefore one should compare their value for t_L with our result for t_D+t_L . These values are similar. They also obtain a hopping matrix element t_{IL} which is smaller than ours by about a factor of 2.5. These differences are probably due to the fact that they include the on-site repulsion energy U_p for the oxygen orbitals. This reduces the energy difference between occupation of vanadium and oxygen orbitals and thus increases the effective hopping between vanadium orbitals.

A strength of our method is that we are able to analyze the origin of particular matrix elements. For example, regarding the similar size of t_D and t_L we find, that it is due to the inclusion of the Na-O hopping elements. Without these we get results as given in the last row of table 10, where t_D is lower than t_L by nearly two orders of magnitude. Similarly, we notice from table 3 that in our model we have more vanadium-oxygen matrix elements than assumed in the tight-binding fit in [9]. As we will see later, this is very important for the determination of the effect of small distortions. There one can no longer use an effective one particle Hamilton operator where only a certain subset of all hoppings is included.

We will next determine the effective superexchange J_{eff} between electrons on neighbouring rungs of the same ladder. We do this by considering the Hamiltonian

$$H = \sum_{i,j} \left(t_{ij}^{VV} a_i^\dagger a_j + h.c. \right) + U \sum_i n_{i\uparrow} n_{i\downarrow} + \sum_{i,j} V_{ij} (n_{i\uparrow} + n_{i\downarrow}) (n_{j\uparrow} + n_{j\downarrow}), \quad (7)$$

where the first term contains the effective hopping between vanadium d_{xy} orbitals as obtained either from LDA or our method. The second term contains the on-site Coulomb interaction U , the last term contains the intersite Coulomb interaction V_{ij} between sites i and j . To determine the effective superexchange we solve this Hamiltonian numerically on a cluster of two neighboring rungs on the same ladder with two d-electrons and set J_{eff} to be the singlet-triplet gap energy on this cluster. We disregard interladder hoppings and we will also disregard the small interlayer hoppings t_c . Now we need values for the onsite Coulomb interaction U and the intersite Coulomb interactions.

Regarding U , it has been estimated in [9] to be 4.0 eV and we will use that value. The intersite Coulomb interaction can be estimated in the following way. As shown in [30] the Hamiltonian for the charge degrees of freedom can be mapped to an antiferromagnetic Ising model in a transverse field. It is well known [31] that in such a model there is a quantum critical point at $2t_R = V_L$ and it has been argued that the material is close to this point [32]. Using $d_L = 3.611$ Å and $d_R = 3.439$ Å we can estimate V_R by assuming that the Coulomb interactions scale with d^{-3} due to screening effects.

The results of our calculation are found in table 10. The estimate from experiment is $0.045 \dots 0.048$ eV [33, 1], which agrees with the results of our calculation. Using the LDA hopping parameters [9] we find a value for J_{eff} from the cluster calculation which is too high. Using the parameters from the ab initio calculation [29] we obtain a J_{eff} which is slightly too low, but better than LDA. Thus, the set of hopping parameters obtained by the above treatment might be preferable for model calculations on the ladders than using the LDA results, especially since the qualitative features regarding t_D and t_L are conserved.

4.2 Hopping and superexchange in the distorted phase

We now repeat the above calculations for the distorted phase: We obtain vanadium-oxygen, oxygen-sodium and vanadium-vanadium hoppings by using the Slater-Koster method. We then project out the vanadium-oxygen and the vanadium-sodium hoppings in the single-particle Hamiltonian to obtain the effective vanadium-vanadium hoppings. We calculate the effective superexchange J_{eff} for the V_1 -ladders as we did for the undistorted phase. However, we now have two inequivalent two-rung-clusters on this ladder due to distortion. The effective superexchange between electrons on neighbouring rungs is different for these two clusters. Therefore we obtain an alternation of J_{eff} along the ladder direction. We did not calculate the effective superexchange for the V_{21} - V_{22} -ladders, since it is strongly modified by charge ordering. [34] All results are found in table 11.

For the V_1 -ladders we find a large alternation of J_{eff} along the ladder with $\delta_J \approx 0.25$, larger by an order of magnitude than we had estimated from the change of the vanadium-oxygen bond lengths. The dimerisation of t_L along the ladder is $\delta_{t_L} \approx 0.2$ and therefore also much larger than what we estimated from the variation of the bond length above. We also note that δ_J and δ_{t_L} are of

Table 11. Effective vanadium-vanadium hoppings t , on-site-energy ϵ and superexchange J_{eff} for the distorted phase given in eV. Denomination of hoppings as given in figure 1. Superexchange J_{eff} has been calculated with $U = 4$ eV, and $V_L = 0.344$ as for the undistorted phase (see text).

Hopping	Layer a	Layer b
V ₂₁ -V ₂₂ -ladders		
$t_{R,CO}$	0.173	0.171
$t_{L,CO}$	0.052	0.057
$t_{D,CO,1}$	0.060	0.061
$t_{D,CO,2}$	0.084	0.086
$t_{cV_{21a}V_{21b}}$		0.015
$t_{cV_{21a}V_{22b}}$		0.010
$t_{cV_{22a}V_{21b}}$		0.005
$t_{cV_{22a}V_{22b}}$		0.004
$\epsilon_{V_{21}}$	1.265	1.250
$\epsilon_{V_{22}}$	1.421	1.428
V ₁ -ladders		
$t_{R,SD}$	0.179	0.180
$t_{L,SD,1}$	0.062	0.068
$t_{L,SD,2}$	0.040	0.046
$t_{D,SD,1}$	0.070	0.070
$t_{D,SD,2}$	0.061	0.061
$t_{c,SD,1}$		0.007
$t_{c,SD,2}$		0.006
ϵ_{V_1}	1.350	1.338
$J_{eff,1}$	0.066	0.072
$J_{eff,2}$	0.038	0.044
δ_J	0.263	0.247
Interladder		
t_{IL1}	-0.081	-0.072
t_{IL2}	-0.130	-0.128

similar size, whereas we would expect a factor of 2 difference from the standard superexchange estimate. The latter fact is, however, easily explained: We estimate the effective superexchange between electrons on neighbouring rungs of the same ladder by looking at the singlet-triplet gap in such a two-rung cluster. This gap essentially describes the kinetic energy gain associated with having the option of locating both electrons on a single site, if they are in a singlet state, whereas they cannot do so if they are in a triplet state. This means that all possible two-particle states contribute to the size of the singlet-triplet gap, including the states where both electrons are on a rung or sitting on the diagonal. Therefore the standard estimate using $J = 4t^2/U$ must fail and this is also the reason for our definition of J_{eff} . This explains why δ_J and δ_{t_L} are of similar size.

The reason for the unexpectedly strong alternation of both J_{eff} and t_L along the V₁-ladder of both layers is more complicated. To understand this we take a closer look at how t_L is actually derived from the original vanadium-oxygen hopping terms and how these change under distortion. Consider hopping along the leg from vanadium site V to V' via the intermediate O₁ as shown in figure 2. The matrix elements are given in table 12. We observe that due to the signs of the hopping elements the

Table 12. Vanadium-oxygen hopping along the leg given in eV. Nomenclature as in figure 2. The first two lines give the hopping for the undistorted phase, the last four lines along the rungs of V_{1a}-ladder in the distorted phase.

	$t_{p_x d_{xy}}$	$t_{p_y d_{xy}}$	$t_{p_z d_{xy}}$
undistorted phase			
VO ₁	-0.8549	0.6303	-0.2470
V'O ₁	0.8549	0.6303	0.2470
distorted phase: layer a			
VO ₁	-0.8486	0.6758	-0.2534
V'O ₁	0.8486	0.6758	0.2534
VO ₃	0.8676	0.5860	0.2358
V''O ₃	-0.8676	0.5860	-0.2358

effective hopping from V to V' via the O₁p_y orbital counteracts the effective hopping via the O₁p_x and the O₁p_z orbital. Thus, in a simple approximation, which neglects all other hoppings taking place in the system, the total effective hopping is

$$t_{VV'} = -\frac{t_{p_x d_{xy}}^2}{\epsilon_V - \epsilon_O} + \frac{t_{p_y d_{xy}}^2}{\epsilon_V - \epsilon_O} - \frac{t_{p_z d_{xy}}^2}{\epsilon_V - \epsilon_O} = -0.250 \text{ eV.} \quad (8)$$

As we can also see from table 12, distortion affects the hoppings via the different oxygen-p-orbitals in a significantly different way. For layer a the dimerisation of these hoppings are approximately $\delta_x = 0.01$, $\delta_y = 0.07$, $\delta_z = 0.04$. But whenever $|t_{p_x d_{xy}}|$ decreases, $|t_{p_y d_{xy}}|$ increases and vice versa. Thus the total dimerisation is enhanced: With the same crude approximation as in equation (8) we obtain $t_{VV'} = -0.207$ eV and $t_{VV''} = -0.294$ eV. This gives a dimerisation of the effective vanadium-vanadium hopping of $\delta_{t_{VV}} = 0.17$. Thus we can explain the very large alternation of the superexchange J_{eff} which we obtained for the V₁-ladders. Thus the main result of the section is that this alternation is almost completely due to the shift of the oxygen atoms on the leg of the V₁ ladders in *a* and *c* direction, and is not caused by the small shift of the vanadium sites.

We can also examine the behaviour of the hopping between layers. For the spin-dimerized V₁ ladders the size of the effective hopping $t_{c,SD}$ changes slightly, but there appears to be no significant alternation in *c* direction. This is different for the effective hopping between charge ordered ladders of neighbouring layers: Hopping is increased between V₂₁ sites and decreased between V₂₂ sites. The size of the effective hopping $t_{c,CO}$ remains very small however, causing a superexchange coupling of less than 1 meV between completely localized electrons on the V₂₁ sites. We conclude that both in the undistorted and the distorted phase all important spin interactions take place within a vanadium-oxygen layer.

5 Summary

In this article we report a structure determination by synchrotron X-ray diffraction of the low temperature phase of α' - NaV_2O_5 . As in [7,12] two slightly different vanadium layers are found to exist as well as two types of two-leg vanadium ladders within each layer. One of these ladders exhibits a zig-zag-type modulation and contains two inequivalent vanadium sites V_{21} and V_{22} . The other ladder contains only one vanadium site V_1 .

Based on the structure determination we perform a bond-valence calculation. Contrary to [8] we find *only two* different valences: the V_{22} and the V_1 sites experience an electron depletion towards a valence of $V^{4.5+\delta}$, while the charge on the V_{21} sites is increased towards a valence of $V^{4.5-3\delta}$. We compare our results with results of a ^{51}V -NMR measurement [6] and find them to be in qualitatively good agreement: Due to charge conservation an asymmetry both in the shift of the two new peaks from the original $V^{4.5}$ peak as well as an asymmetry in intensity are found.

We then use a Slater-Koster treatment to find the hopping along the bonds and project out the V-O and V-Na processes to obtain effective vanadium-vanadium hoppings. The results compare well with LDA [9] as well as ab initio calculations [29] regarding relations between the different matrix elements on the ladder. When we calculate the effective superexchange between rungs for the undistorted phase using our matrix elements we find a value of 0.047 eV which compares well with experimental results of 0.045...0.048 eV. In the distorted phase we obtain a strong alternation of the superexchange with dimerisation $\delta_J \approx 0.25$ in the V_1 ladders along ladder direction. This dimerisation is nearly exclusively due to the shift of the oxygen atoms mediating the hopping along the legs of the ladders in a and c direction; the shift of the vanadium atoms is much smaller. Even though the Slater-Koster method is known to overestimate the effect of small distortions, the results show clearly, that a significant alternation of the superexchange is taking place on the V_1 -ladders. No alternation in b-direction is found for the V_{21} - V_{22} ladders. No significant hopping or superexchange between layers is found both for the undistorted and the distorted phase.

This leaves the question of the origin of the spin gap which has been observed in the material. According to our results for the valence of the different vanadium sites the picture of spin-singlet clusters proposed in [12] cannot be correct, since it relies heavily on having V^{5+} sites in the distorted phase. However, in ^{23}Na -NMR eight inequivalent sodium sites have been detected [18,10]. In our structure determination we obtain only six inequivalent sites. Four of these sites are located above and below the spin dimerised V_1 -ladders, two of them are located above and below the charge-ordered V_{21} - V_{22} -ladders. To have eight inequivalent sodium sites it would be sufficient to assume, that along the V_{21} - V_{22} -ladders the shift of equivalent sodium sites in c direction alternates along the ladder direction. This would also immediately imply an alternation of the superexchange on the charge-ordered ladders, since, as we have shown above, the hopping via the sodium

site is crucial to explain the diagonal hopping between two rungs of the same ladder. Alternatively, such an alternation of inequivalent sodium atoms can result from an alternating shift of the rung oxygens of the V_{21} - V_{22} -ladders in b direction. This would also cause a superexchange alternation along the V_{21} - V_{22} -ladders and one would also have eight inequivalent sodium sites in the system. Such shifts would explain in a simple manner both the observation of ^{23}Na -NMR and the existence of a spin gap without disagreeing so far with the results of all X-ray structure determinations. Since the superexchange alternation seems to be much stronger on the V_1 -ladders, this would imply a system with two significantly different spin gaps.

Another explanation for the observation of eight inequivalent sodium sites has been given in [10]. The authors propose that a charge ordering takes place on all ladders. However, this implies having eight inequivalent sites provided, one has a) an alternation of sodium sites along the ladder direction, thus implying superexchange alternation as above for the case of the V_{21} - V_{22} -ladders, b) two inequivalently charge ordered ladders. If one had the same amount of charge ordering on both ladders one would also expect the same sodium sites, since charge/valence and bonds are strongly related. So, in such a case, four inequivalent vanadium sites would have to be observed in ^{51}V -NMR, which is not the case [6].

In conclusion we have done a structure determination of the low temperature phase of α' - NaV_2O_5 . We confirm the results of [7,12], having charge ordered V_{21} - V_{22} -ladders and disordered V_1 -ladders. However, a bond valence calculation using our results finds only two instead of three significantly different valences: The valence of the V_1 and the V_{22} sites turns out to be nearly the same. By making use of the Slater-Koster method we find a strong alternation of the superexchange coupling between rungs of the V_1 -ladders.

T. C. would like to thank Dr. H.-G. Krane for his help doing synchrotron X-ray measurements.

References

1. Isobe M., Ueda Y., J. Phys. Soc. Jpn. **65**, (1996) 1178
2. Carpy A., Galy J., Acta Crystallogr. Sect. B **31**, (1975) 1481
3. von Schnering HG., Grin Y., Kaupp M., Somer M., Kremer R.K., Jepsen O., Chatterji T., Weiden M., Z. Kristallogr. NCS **213**, (1998) 246
4. Meetsma A., de Boer J.L., Damascelli A., Jegoudez J., Revcolevschi A., Palstra T.T.M., Acta Crystallogr. Sect. C **54**, (1998) 1558
5. Smolinski H., Gros C., Weber W., Peuchert U., Roth G., Weiden M., Geibel C., Phys. Rev. Lett. **80**, (1998) 5164
6. Ohama T., Yasuoka H., Isobe M., Ueda Y. Phys. Rev. B **59**, (1999) 3299
7. Lüdecke J., Jobst A., van Smaalen S., Morre E., Geibel C., Krane H.G., Phys. Rev. Lett. **82**, (1999) 3633
8. van Smaalen S., Lüdecke J., Europhys. Lett. **49**, (2000) 250

9. Yaresko A. N., Antonov V. N., Eschrig H., Thalmeier P., Fulde P., Phys. Rev. B **62** (2000)
10. Ohama T., Goto A., Shimizu T., Ninomiya E., Sawa H., Isobe M., Ueda Y., J. Phys. Soc. Jpn. **69** (2000) 2751
11. Chatterji T. *et al.*, to be published
12. de Boer J.L., Meetsma A., Baas J., Palstra T.T.M., Phys. Rev. Lett **84**, (2000)3962
13. Nakao H., Ohwada K., Takesue N., Fujii Y., Isobe M., Ueda Y., Sawa H., Kawada H., Murakami Y., David W.I.F., Ibberson R.M., Physica B **241–243**, (1997) 534
14. Brown I. D., Shannon R. D. Acta Cryst. Sect. A **29**, (1973) 266
15. Brown I. D., Altermatt D., Acta Crystallogr. Sect. B **41**, (1985) 244
16. Brown I. D., Acta Cryst. B **48** (1992) 553
17. Horsch P., Mack F., Europhys. J B **5** (1998) 367
18. Fagot-Revurat Y., Mehring M., Kremer R. K., Phys. Rev. Lett. **84**, (2000) 4176
19. Sherman E.Y., Fischer M., Lemmens P., van Loosdrecht P.H.M., Guntherodt G., Europhys. Lett. **48**, (1999) 648
20. Hirota K., Cox D.E., Lorenzo J.E., Shirane G., Tranquada J.M., Hase M., Uchinokura K., Kojima H. Shibuya Y., Tanaka I., Phys. Rev. Lett. **73**, (1994) 736
21. Johnston D.C., Kremer R.K., Troyer M., Wang X., Klumper A., Bud'ko S.L., Panchula A.F., Canfield P.C. Phys. Rev. B **61**, (2000) 9558
22. Konstantinovic M.J., Ladavac K., Belic A., Popovic Z.V., Vasil'ev A.N., Isobe M., Ueda Y., J. Phys. Cond. Mat. **11**, (1999) 2103
23. Lohmann M., Loidl A., Klemm M., Obermeier G., Horn S., Sol. Stat. Comm. **104**, (1997) 649
24. Vasilev A.N., Smirnov A.I., Isobe M., Ueda Y., Phys. Rev. B **56**, (1997) 5065
25. Hase M., Terasaki I., Uchinokura K., Phys. Rev. Lett. **70**, (1993) 3651
26. Honecker A., Brenig W., Phys. Rev. B **63**, (2001) 4416
27. Harrison W. A., *Electronic structure and the properties of solids* (Dover, 1989)
28. Slater J. C., Koster G. F., Phys. Rev. **94**, (1954) 1498
29. Suaud N., Lepetit M.-B., Phys. Rev. B **62** (2000) 402
30. Thalmeier P., Fulde P., Europhys. Lett. **44** (1998) 242
31. Pfeuty P., Annals of Phys. **57**, (1969) 79
32. Mostovoy M.V., Knoester J., Khomskii D.I., cond-mat/0009464
33. Mila F., Millet P., Bonvoisin J., Phys. Rev. B **54** (1996) 11925
34. Yushankhai V., Thalmeier P., Phys. Rev. B **63** (2001) 4402